Gold nanoparticles as scaffolds for poor water soluble and difficult to vehiculate antiparkinson codrugs

A Di Crescenzo,[1] **I Cacciatore**,[1] **M Petrini**,[2] **M D'Alessandro**,[2,3] **N Petragnani**,[4] **P Del Boccio**,[2,3] **P Di Profio**,[1] **S Boncompagni**,[5] **G Spoto**,[2] **H Turkez**,[1,6] **P Ballerini**,[4] **A Di Stefano**[1] **and A Fontana**[1,*]

[1] Department of Pharmacy, University "G. d'Annunzio", Chieti I-66100, Italy

[2] Department of Medical, Oral and Biotechnological Sciences, University "G. d'Annunzio", Chieti I-66100, Italy

[3] CeSI - Center for Research on Ageing, University "G. d'Annunzio", Chieti I-66100, Italy

[4] Department of Psychological, Health and Territorial Sciences, University "G. d'Annunzio", Chieti I-66100, Italy

[5] DNICS – Department of Neuroscience, Imaging and Clinical Sciences, University "G. d'Annunzio", Chieti I-66100, Italy

[6] Department of Molecular Biology and Genetics, Erzurum Technical University, Erzurum 25240, Turkey

E.mail: antonella.fontana@unich.it

Abstract. We report the facile and non-covalent preparation of gold nanoparticles (AuNPs) stabilized by an antiparkinson codrug based on lipoic acid (**LA**). The obtained AuNPs appear stable in both DMSO and fetal bovine serum and able to load an amount of codrug double the weight of gold. These NPs demonstrated to be safe and biocompatible towards primary human blood cells and human neuroblastoma cells, one of the most widely used cellular model to study dopaminergic neural cells, therefore ideal drug carriers for difficult to solubilize molecules. Very interestingly, the codrug-stabilized AuNPs demonstrated to reduce the accumulation of ROS in SH-SY5Y cells treated with **LD** and did not change TOS levels in cultured human blood cells, thus confirming the antioxidant role of **LA** although bound to AuNPs. The characterization of AuNPs in terms of loading and stability paves the way to their use in biomedical and pharmacological applications.

1. Introduction

The progress in Parkinson's disease (PD) therapy is mainly focused on codrug approach [1]. To overcome the pro-oxidant effect associated with L-Dopa (**LD**) therapy, recently, new codrugs with antioxidant and iron-chelating properties have been synthesized, by joining **LD** and dopamine (**DA**) with (R)-alpha-lipoic acid (**LA**) [2] (Figure 1).

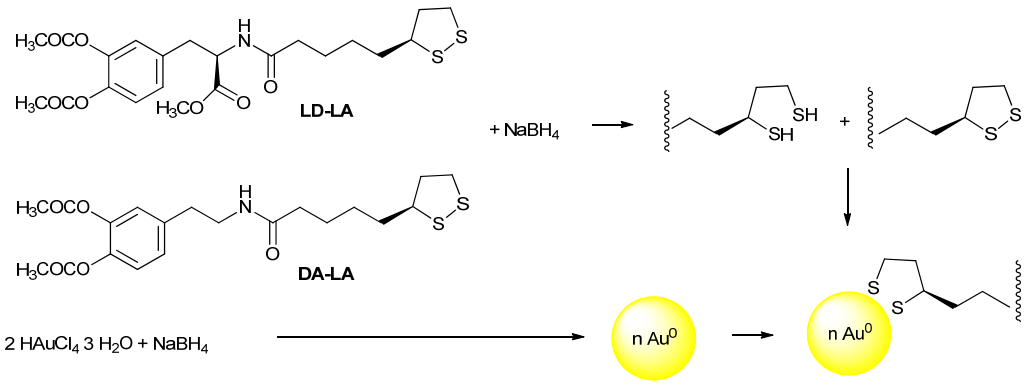

Figure 1. Scheme of reactions involved in the preparation of coated AuNPs.

LA is a natural and essential cofactor for mitochondrial bioenergetic enzymes and it has been already proposed as a therapeutic agent for chronic diseases associated with oxidative stress [3,4]. Recently, in the biomedical field gold nanoparticles are receiving much attention due to their potential applications in targeted delivery of drugs [5,6] and optical bioimaging [7].

The gold nanoparticles (AuNPs), as well as being inert and non-toxic [7,8], can be easily synthesized with a reproducible process [7] in order to provide a monodisperse population. Their surface can be easily conjugated with ligands of different nature, but those widely used and investigated are thiols which exploit the strong Au–S bond between the soft acid Au and the soft thiolate base [9]. For this reason **LA**, characterized by the presence of a disulfide group S-S, is particularly promising for acting as AuNP stabilizer, as it can theoretically furnish a twin thiolate anchor to the NPs. In the literature a few examples of **LA** used as an efficient bridge to immobilize molecules on gold nanoparticles have already been published [10-13]. In such a context, Legname et al. proposed the use of gold nanoparticles in the treatment of neurodegenerative diseases caused by protein aggregates (e.g. Lewy's bodies for the PD) as carriers able to cross the blood-brain barrier (BBB) [14].

The aim of the present work is the synthesis and the functionalization of gold nanoparticles with **LD-LA** and **DA-LA** codrugs and their characterization in terms of dimensions, morphology and stability. A thorough study has been performed to determine the gold/codrug ratio which can ensure the optimal control of nanoparticle size and loading capacity. Differently from recently used polymeric nanoparticles [15] or liposomes [16,17], these carriers do concentrate a higher amount of drug per nanoparticle thank to the fact that the drug is adsorbed outside rather than solubilized inside the nanoparticle thus ensuring high concentration of hydrophobic drugs in the blood vessels. Besides, the presence of the drugs on the AuNPs surface, due to the activation of specific membrane transporters [14] for **DA** and **LA**, may ensure high permeability and result in high biodistribution, developing long acting formulations in order to provide continuous dopaminergic stimulation (CDS) [19]. In addition, the safety and biocompatibility of synthesized **LD-LA**/AuNPs were tested in SH-SY5Y human neuroblastoma cells, one of the most widely used cellular model to study dopaminergic neural cells, and in cultured primary human blood cells.

2. Experimental Section

2.1. Materials

Hydrogen tetrachloroaurate (III) trihydrate ($HAuCl_4 \cdot 3\ H_2O$) 99.99% and sodium borohydride ($NaBH_4$) were purchased from Alfa-Aesar. Dimethyl sulfoxide (DMSO) for UV-Spectroscopy > 99.8% and Sephadex® G-25 were purchased from Sigma-Aldrich. All reagents were used without further purification. Fetal bovine serum (FBS) and phosphate buffer (PBS) were purchased from EuroClone, Milan (Italy).

2.2. LD-LA and DA-LA synthesis

LD-LA and **DA-LA** were synthesized according to ref. [2].

2.3. Preparation of gold nanoparticles

A few microliters of a concentrated solution of tetrachloroauric acid in DMSO were added to a round-bottom flask and diluted with DMSO in order to obtain a final volume of 5 mL and the desired final concentration of Au. The solution was added with a few microliters of a concentrated DMSO solution of the codrug and stirred at a speed of 600 RPM with a magnetic bar for 30 minutes. At this point, few microliters of a concentrated freshly-prepared solution of sodium borohydride in DMSO were added to the solution. Finally, AuNPs were purified by gel permeation through Sephadex® G-25. The amount of the added reagents controls the size of the gold nanoparticles as reported in the Results and Discussion Section (see below). The reaction, whose progression was followed by the color change of the solution, was left stirring for 24 h preferably in the dark (see Figure 1).

2.4. In vitro release study in phosphate buffer pH 7.4

In vitro release study was performed using the dialysis bag method [20, 21]. In detail, 1 mM **LD-LA**/AuNPs was diluted 1:10 with phosphate buffer pH 7.4 (BPS), poured into the dialysis bag, and placed in a shaker, at 37 °C and 100 rpm, containing the medium (PBS buffer pH 7.4). At exact time intervals, fractions of the nanoparticulate suspension were collected from the bag, diluted with organic solvent, and assayed for the codrug content by HPLC coupled with electrochemical detection. The percentage of **LD-LA** released from nanoparticles was calculated through an indirect method by the following equation:

$$\% \text{ released codrug} = 100 - \% \text{ remaining codrug}$$

2.5 Stability of codrug-coated AuNPs

Stability of 1.0 mM **LD-LA**/AuNPs and 1.0 mM **DA-LA**/AuNPs in DMSO was investigated over the time by monitoring the UV-vis spectrum of a 1.0 mM codrug/AuNPs DMSO solution for 15 weeks. Stability of 1.0 mM **LD-LA**/AuNPs in PBS was monitored over the time by diluting the 1.0 mM DMSO **LD-LA**/AuNPs solution 1:10 with PBS and using both UV-vis spectrophotometry and dynamic laser light scattering. The stability of 1.0 mM **LD-LA**/AuNPs in fetal bovine serum (FBS) was monitored over the time by diluting the 1.0 mM DMSO **LD-LA**/AuNPs solution 1:10 and 1:100 with FBS. Due to the presence of proteins in FBS, only dynamic laser light scattering was used for this latter determination.

2.6. Preparation of primary human whole-blood, isolated lymphocyte and human SH-SY5Y neuroblastoma cell cultures

2.6.1. Subject and sample collection. Venous blood was taken from each of four healthy, male donors using sterile heparinized tubes from 23-27 years old non-smoking donors, not exposed to radiation, drugs or any antioxidant supplementation in the recent past.

2.6.2. Cell cultures. Human peripheral whole-blood cultures were set up according to a minor modification of the protocol as previously reported by Evans and O'Riordan [22]. The heparinized whole-blood (0.5 mL) was cultured in 6 mL culture medium (Chromosome Medium B, Biochrom, Leonorenstr. 2-6, D-12247, Berlin) with 5 μg/L of phytohemagglutinin (Biochrom). Likewise, the isolated lymphocyte cultures were set up after lymphocyte isolation with Ficoll centrifugation. After supplementation with different concentrations (10, 50 and 100 μg/mL) of **LD-LA**/AuNPs or **LD-LA** (dissolved in DMSO), the whole-blood and isolated lymphocyte samples were incubated for 24 and 48 h at 37 °C to adjust body conditions. Experiments conformed to the guidelines of the World Medical Assembly, Declaration of Helsinki [23]. The cultures without compounds were studied as negative control group. 0.1% Triton X-100 was used as the positive control in MTT and LDH assays. Likewise, ascorbic acid (10 μM) and hydrogen peroxide (25 μM) were also used as the positive controls in TAC and TOS analysis, respectively.

2.6.3. Human SH-SY5Y neuroblastoma cell cultures. Undifferentiated SH-SY5Y, human neuroblastoma cells, were a kind gift of Prof. M. Reale, University of Chieti, Italy and were maintained in DMEM medium (Sigma-Aldrich S.r.l., Milan, Italy) containing 10% heat inactivated FBS, 2 mM L-Glutamine and 1% penicillin/streptomycin (Life Technologies Italia, Monza, Italy) at 37 °C with 5% CO_2. Culture medium was changed every 2-3 days. SH-SY5Y cells (70–75% confluent) were incubated with different concentrations of **LD**, **LD-LA** or **LD-LA**/AuNPs (dissolved in DMSO) for 24 and 48 h at 37 °C.

Great care was taken in maintaining the cells in an undifferentiated state, preventing them to reach confluence and using them within few culture passages [24].

2.7. Bioassey

2.7.1. MTT assay. Cell viability was evaluated by MTT assay based on the reduction of MTT, a yellow tetrazole, to purple insoluble formazan by mitochondrial respiration in viable cells. MTT assay was performed on SH-SY5Y cells and on cultured lymphocytes (10.000 cells/well into flat-bottom 96-well plates) after different incubation durations (24 or 48 h) in the presence or in the absence of the drugs to be tested. Lymphocytes were precipitated by centrifugation and washed twice by phosphate buffer whereas SH-SY5Y cells were washed twice by phosphate buffer. Then, 50 µL of MTT solution was added and cells were incubated for 4 h at 37 °C. At the end, 125 µL of DMSO solution was added and the absorbance was determined at 570 nm by ELISA reader (SpectraMax1 190, Molecular Devices, UK). The viability of the treatment groups was shown as the percentage of negative controls assumed to be 100%.

2.7.2. Lactate dehydrogenase (LDH) release assay. LDH released from damaged cells in whole-blood culture medium and in SH-SY5Y cell (10.000 cells/well into flat-bottom 96-well plates) culture medium was quantified using LDH assay kit (CytoTox 96® Non-Radioactive Cytotoxicity Assay, Promega, Milan, Italy or Cayman Chemical Co. Ann Arbor, Michigan, USA). Released LDH catalyzed the oxidation of lactate to pyruvate with simultaneous reduction of NAD^+ to NADH, which is detected by colorimetric assay. The cells were treated with **LD**, **LD-LA** or **LD-LA**/AuNPs (dissolved in DMSO) and incubated for 24 or 48 h. To measure the positive control, 15 min before the treatments end 10 µL of positive control reagent were added to 3 wells. Fifty µL of medium were taken, added of 50 µL of substrate reagent and incubated for 30 min at RT. To stop the reaction, 50 µL of stop solution were added and absorbance at 490 nm was read using a micro plate reader (SpectraMax1 190, Molecular Devices, UK or Biotek Instruments Inc., Winooski, VT).

Cell viability was calculated with equation (1):

$$Cell\ viability = 100 - \left(\frac{Abs_{490}}{CTRL^{+}Abs_{490}} * 100\right) \quad \text{(eq. 1)}$$

2.7.3. Intracellular reactive oxygen species (ROS) measurement. An assay based on the conversion of non-fluorescent DCFH2-DA to a fluorescent species by intracellular ROS was used in this study (DCFDA Cellular ROS Detection Assay Kit, Abcam, Prodotti Gianni S.p.A., Milan, Italy). SH-SY5Y cells (25.000 cells/well) were seeded in 96-well black-bottom plates and left to adhere for 48 h. Cells were rinsed with PBS 1× and

loaded with 50 μM DCFH2-DA for 45 min at 37 ℃ in the dark, the cells were then washed twice with the same buffer and treated with different concentrations of **LD**, **LD-LA** or **LD-LA**/AuNPs (dissolved in DMSO) for 24 h at 37 °C. After exposure to the compounds, the cells were washed with PBS 1× and fluorescence intensity was measured (λ_{exc} 485 nm / λ_{em} 535 nm) using a fluorescence spectrophotometer (SpectraMax1 190, Molecular Devices, UK). To measure the positive control, 2 h before the treatments end *tert*-butyl hydrogen peroxide (TBHP) 50 μM were added to positive control wells. ROS production was expressed as percent of positive control, following equation (2):

$$ROS\ production = \frac{FAU}{FAU_{CTRL}} * 100 \quad \text{(eq. 2)}$$

where FAU is Fluorescence Arbitrary Units.

2.7.4. TAC and TOS analysis. The automated total antioxidant capacity and total oxidant status assays were carried out in plasma samples obtained from whole-blood cultures for 24 and 48 h by commercially available kits (Rel Assay Diagnostics®, Turkey).

2.8. Statistics

Statistical analysis was performed using SPSS Software (version 18.0, SPSS, Chicago, IL, USA). For statistical analysis of obtained biological data Duncan's test was used. Statistical decisions were made with a significance level of 0.05.

3. Results and discussion

3.1. Synthesis of the gold nanoparticles

The aim of the present study was to favour the vehiculation and the preparation of highly concentrated lipoic acid derived-codrugs by exploiting their disulfide group in order to prepare thiol-stabilized gold nanoparticles. Indeed either the disulfide group as it is or the double functionalized thiolate moiety obtained by reduction of the disulfide group of **LA** may adsorb onto, and stabilize, AuNPs [25]. The most popular preparation protocol for hydrophobic thiol-stabilized gold nanoparticles is the well known two-phase Brust-Schiffrin method [26]

published in 1994. The preparation protocol proposed therein demonstrated to allow the synthesis of stable and size-controlled AuNPs. Nevertheless, this method makes use of toxic toluene solvent and tetraoctylammonium bromide used as the phase-transfer reagent. For this reason, with the aim of making the preparation procedure more biocompatible and simplify its protocol, we modified the one-phase preparation protocol proposed by the same Authors one year later [27]. Several other studies [12,13] reported the use of bidentate anchoring groups for the formation of AuNPs, but in the present study we improved the system by stabilizing the AuNPs with molecules, such as **LA** and **LD**, that, besides being active in the PD therapy, demonstrated [18] to activate specific amino-acid membrane transporters.

3.1.1. Use of $NaBH_4$ as the reducing agent. The selected protocol envisages the use of $NaBH_4$ as the reducing agent. First of all, we checked whether this reagent was able to reduce the disulfide bond of the lipoic portion of the codrug as well as Au^{3+} to Au^0. Evidences of disulfide reduction by $NaBH_4$ in aqueous solutions [28] and organic solvent mixtures [29] had already been reported and demonstrated to strongly depend of the disulfide structure [29]. Under the adopted conditions and $NaBH_4$ concentration, the investigated drugs were partially reduced. In particular, from the reported molar extinction coefficient of disulfide bond at 337 nm, it seemed that 3.1%, 48% and 20% of **LD-LA**, **DA-LA** and the reference **LA** reduced to the relevant thiols or thiolate, respectively (see Figure S1 in the Supplementary data). It is important to note that in the presence of Au^{3+} the stoichiometric amount of $NaBH_4$ available for disulfide reduction decreases to 0.5 equivalents (see Figure S2 in the Supplementary data). Therefore, thiols, thiolate and disulfide adsorb on the gold surface in agreement with previous studies that reported a strongly favoured but not exclusive formation of thiolate-Au interactions via dissociation of the disulfide over S-H bond cleavage associated to much weakly (namely ca. 20 kcal/mol) bound disulfide-Au [30,31].

$NaBH_4$ has been chosen because it is a weak reducing agent that should promote reduction of both disulfide and Au^{3+}, without altering other functional groups present in the reaction mixture, (i.e. esters). Actually, we found that both codrugs are partially hydrolyzed under the experimental conditions. In particular, the increase of the absorbance of the peak at 287 nm, associated to **LD** in DMSO (Figure S3 in the Supplementary data), evidenced that, after 24 h, at least 50% of **LD-LA** hydrolyzed to **LD** on addition of an excess $NaBH_4$ (1.5 eq) (Figure S4 in

the Supplementary data). Despite this percentage should reduce strongly when $HAuCl_4$ is present in the reaction mixture, the partial hydrolysis of **LD-LA** does not affect the activity of the codrug [32]. On the other hand, **DA-LA** appeared to degrade more easily (i.e. the spectrum changed immediately on addition of $NaBH_4$) and the increase of **DA** absorption at λ 286 nm (see Figure S5 in the Supplementary data) allowed to monitor, after 24 h (see Figure S6 in the Supplementary data), a slightly higher percentage of degradation on addition of excess $NaBH_4$ with respect to **LD-LA**. This behavior is probably due to the higher nucleophilicity of the amino group of **DA** as compared to that of **LD**. We thus concentrated our further studies of drug quantification and biocompatibility analyses only on **LD-LA** although **DA-LA** demonstrated to be equally able to stabilize AuNPs, as reported below. The DMSO proved to be the ideal solvent because it is able to solubilize very well all of the reagents and products. Furthermore, due to its low toxicity and ability to cross biological membranes, it is approved as an efficient pharmaceutical eccipient [33].

3.1.2. Sequence of addition and ratio of the reagents. In order to reduce the possible degradation of the codrug and to maximize the reduction of the $HAuCl_4$, we added the reducing agent directly to the mixture of oxidized codrug and $HAuCl_4$ under an effective and constant stirring speed of 600 RPM. Table 1 lists samples of gold nanoparticles obtained with different concentrations of reducing agent, while keeping the concentrations of $HAuCl_4$ and codrug constant. As reported in Table 1, both concentrations of $NaBH_4$, 1 and 1.5 mM, allowed to obtain small AuNPs, with 1.5 mM being the best choice for both codrugs because it yielded AuNPs with diameters less than 6 nm. Higher concentrations of $NaBH_4$ have not been investigated due to the recently demonstrated capability of $NaBH_4$ to act as ligand removal reagent for AuNP surfaces [34].

Table 1. Samples of gold nanoparticles obtained with the **LD-LA** and **DA-LA** codrugs, with concentrations of codrug and $HAuCl_4$ of 1 mM, varying the concentration of $NaBH_4$.

Entry	Codrug	[$NaBH_4$] (mM)	Size[a] (nm)
1	**LD-LA**	1.0	8.1±0.3
2	**LD-LA**	1.5	3.8±0.3
3	**DA-LA**	1.0	10.1±0.3

4	**DA-LA**	1.5	5.7±0.3

[a] Determined by DLS. All of the data were a mean of at least two measurements.

In order to confirm NP dimensions we checked AuNPs size by exploiting TEM measurements. In fact, data acquired by using DLS refers properly to hydrodynamic rather than real diameters and it is known [12] that, in the presence of not monomodal NP populations, weak scattering of smaller NPs can be hampered by the scattering of the larger NPs. TEM micrographs reported in Figure 2 showed that the gold nanoparticles were spherical in shape, morphologically uniform, well separated from each other and with an average diameter of around 2 nm.

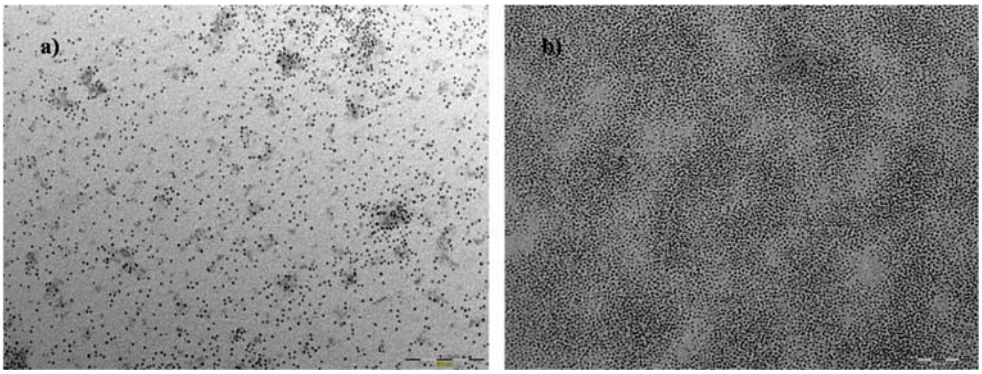

Figure 2 TEM images of gold nanoparticles functionalized with codrug **LD-LA** (a) and with **DA-LA** (b). Concentration used: $HAuCl_4$ 1 mM, $NaBH_4$ 1.5 mM, codrug 1 mM. Scale bar: 100 nm.

The optimization of the concentration of the codrug was performed by keeping the concentration of other reagents constant. Data reported in Table 2 show that in the range of concentrations examined a strong correlation between the concentration of the codrug and the size of the obtained AuNPs was not observed. Small-sized gold nanoparticles could be recovered at all the investigated concentrations of codrugs. The only exceptions were samples with drug concentrations higher than 3 mM. It is likely that a high codrug concentration depleted $NaBH_4$ thus decreasing Au^{3+} reduction, or that a different ratio of pure codrug/reduced prodrug/degraded prodrug decreased its capacity to act as a good stabilizer due to a change of codrug solubility and/or affinity for the NP.

Table 2. Gold nanoparticles obtained by varying the concentration of the two codrugs **LD-LA** and **DA-LA**, while keeping the concentrations of $HAuCl_4$ and $NaBH_4$ constant at 1 mM and 1.5 mM, respectively.

Entry	Codrug	[Codrug] (mM)	Size[a] (nm)	λ_{max} interval[b] (nm)
1	**LD-LA**	0.10	5.9±0.5	516-518
2	**DA-LA**	0.10	5.3±0.6	517-520
3	**LD-LA**	0.25	5.8±0.5	516-524
4	**DA-LA**	0.25	5.7±0.3	516-520
5	**LD-LA**	0.50	6.7±0.6	518-522
6	**DA-LA**	0.50	6.1±0.5	519-521
7	**LD-LA**	0.75	4.2±0.3	512-519
8	**DA-LA**	0.75	4.7±0.3	515-520
9	**LD-LA**	1.00	4.2±0.2	515-520
10	**DA-LA**	1.00	4.3±0.1	515-520
11	**LD-LA**	1.50	7.0±0.8	517-521
12	**DA-LA**	1.50	5.5±0.4	517-520
13	**LD-LA**	2.0	5.3±0.3	512-519
14	**DA-LA**	2.0	8.4±0.7	510-523
15	**LD-LA**	3.0	5.2±0.3	510-519
16	**DA-LA**	3.0	140±4.2	512-530
17	**LD-LA**	5.0	5.2±0.5	516-522
18	**DA-LA**	5.0	143±5.8	529-532

[a] Determined by DLS. All of the data were a mean of at least two measurements. [b] The λ_{max} interval is calculated considering an absorbance change of ±0.0015 a.u.

DLS data are partly confirmed by spectrophotometric analyses. As a matter of fact, gold nanoparticles with spherical shape and dimensions ranging between 3 and 10 nm showed an absorption plasmon band at a wavelength of about 520 nm whose position and shape depend of the size, shape and distance among the particles. Aggregates of gold nanoparticles show Plasmon bands at wavelengths higher than 520 nm [35]. Similarly, the growth of gold nanoparticles size results in an absorption band shift towards the near infrared spectral region [35], although binding events occurring at the surface can significantly affect the peak wavelength [36]. In the present case the plasmon absorption bands are relatively large (see Figure S7 in the Supplementary data) and size difference are relatively low, therefore only a rough correlation can be observed between the size of the synthesized gold nanoparticles and the wavelength of the Plasmon absorption band. Perhaps this is due to the fact that the AuNPs surface is non-homogenously coated with the stabilizing agents and different binding events at the surface can affect the correlation. Samples characterized by diameters as large as 10 nm have a maximum absorption wavelength at *ca.* 520 nm, the only exceptions being entries 16 and 18, probably due to not monomodal NP populations or aggregation of NPs as evidenced by the high hydrodynamic value monitored in those cases. A good correlation was instead evaluated by considering the simple and fast method based on UV-vis spectrophotometry and multiple scattering theory associated with correction of the complex refraction index of the gold nanoparticles, proposed by Haiss and intended to determine the size and concentration of gold nanoparticles [37,38]. As a matter of fact, for AuNPs obtained by using 1 mM **LD-LA** and **DA-LA** a diameter of 2.28 and 2.22 nm can be calculated (see relevant UV-vis spectra in Figure S7 in the Supplementary data). With regard to the reaction time, although gold nanoparticles with selected characteristics are obtained sometimes even after 12 h, we choose to prolong the reaction to 24 h. Reaction times longer than 24 h (i.e. 48 h) led to the formation of larger nanoparticles (see Table S1 in the Supplementary data).

3.2. Comparison with LA

Samples of gold nanoparticles obtained with both the codrugs were compared with samples of gold nanoparticles obtained with **LA**. A first difference between the various samples is easily observable by the naked eye, because the solutions of the samples with **LA** appear lighter, as shown in Figure 3. Gold nanoparticles with **LA** were

obtained under the same reaction conditions of the other samples, with reducing agent 1.5 mM and $HAuCl_4$ 1 mM. Table 3 reports size and wavelength of the samples obtained with various concentrations of **LA** (Figure S8 in the Supplementary data reports the relevant UV-vis spectra). Similarly to the **LD-LA** and **LD-LA**/AuNPs samples, only a broad correlation can be observed between the size of the synthesized gold nanoparticles and the wavelength of the Plasmon absorption band for the reasons mentioned above.

Table 3. Samples of **LA** obtained with $HAuCl_4$ 1 mM, $NaBH_4$ 1.5 mM and increasing concentration of **LA**.

Entry	[**LA**] (mM)	Size[a] (nm)	λ_{max} interval[b] (nm)
1	0.10	10.1±0.4	519-524
2	0.25	5.6±0.3	511-523
3	0.50	11.2±0.5	517-525
4	0.75	5.1±0.1	518-520
5	1.00	6.6±0.2	512-522
6	1.50	13.0±0.4	515-524
7	2.00	6.2±0.3	518-521
8	3.00	11.4±0.4	522-527
9	5.00	10.2±0.6	521-527

[a] Determined by DLS. All of the data were a mean of at least two measurements. [b] The λ_{max} interval is calculated considering an absorbance change of ±0.0015 a.u..

Figure 3. Samples of gold nanoparticles prepared with **LD-LA** (right), **LA** (center), **DA-LA** (left). For each couple the concentration of the drug/codrug is 1.0 mM in the left vial and 2.0 mM in the right vial.

3.3. Evaluation of drug loading

In view of the potential biopharmaceutical applications, it is essential to evaluate the concentration of the drug administered and therefore the number of the codrug molecules adsorbed on each nanoparticle. As reported above, our study evidenced that the variation of the concentration of the codrug (in the investigated range) does not strongly affect the particle size due to the fact that we worked in excess of stabilizer (i.e codrug). This means that not all the molecules of the codrug used during the preparation of the nanoparticles have been adsorbed onto the gold surface and that some are free in solution. Therefore, we first removed codrug excess by gel filtration. Once codrug excess was removed, we determined the amount of the adsorbed codrug. We decided to exploit the HPLC-ESI-MS/MS technique (High Performance Liquid Chromatography – electrospray tandem mass spectrometry). After setting the optimal MRM (multiple reaction monitoring) operating conditions for our analytes, as reported in the Experimental section, we quickly found that there was no difference between the **LD-LA** alone and that bound to the nanoparticles in terms of retention time (i.e. 14.6 min). Likely, the bond between S and Au did not withstand the adopted separation conditions and, due to the large affinity of codrugs and **LA** for the used solvents (i. e. acetonitrile and methanol) and stationary phase [39], most of the stabilizing agent tended to desorbe from the NPs and entered the electrospray mass spectrometer already separated from NPs. In order to evaluate the amount of **LD-LA** adsorbed onto the AuNPs (see Supplementary data) we thus compared the LC-MS/MS signal of the filtered with that of the unfiltered sample (See Figure S9 in the Supplementary

data). From calculations based on the areas of the chromatographic peaks and the amount of reagents used, we calculated that each gold nanoparticle bound 41 molecules of **LD-LA**. This ratio appears quite low as compared to similar systems [11] and for this reason we determined further the same ratio (molecules of **LD-LA** per NP) by performing thermogravimetric analysis (see Figure 4), i.e. the classic and most widely used method to determine the percentages of the components in such nanohybrids. After an initial slow heating phase at 120 °C, the loss in weight on increasing the temperature for both the pure codrug **LD-LA** and the hybrid **LD-LA**/AuNPs were recorded.

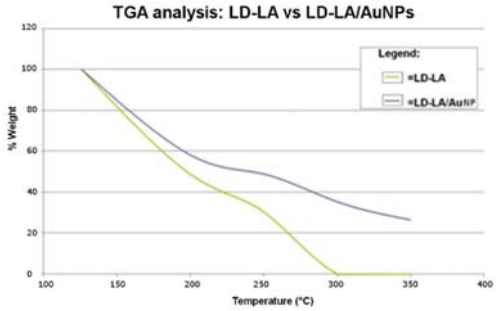

Figure 4. Thermogravimetric analysis curves measuring the loss of organic material for neat **LD-LA** (green line) and **LD-LA**/AuNPs obtained with $HAuCl_4$ 1 mM, $NaBH_4$ 1.5 mM and **LD-LA** 1 mM (blue line).

The thermogram in Figure 4 showed that at around 300 °C the combustion of neat **LD-LA** was almost complete. This result is plausible if we consider the features of the two components of the codrug: **LD** has a melting point of 295 °C, whereas **LA** is decomposed at lower temperature (> 60 °C). The curve relating to the hybrid **LD-LA**/AuNPs highlighted a weight loss of 64.75% ascribable to **LD-LA** and a residue of 35.25% (i.e. Au). In a second experiment the corresponding values were 71.36% and 28.64%. Based on these results and the calculations reported in the Supplementary data (See Section 11, TGA Analyses), it might be inferred that a gold nanoparticle had approximately 185 **LD-LA** molecules adsorbed on its surface. Two different measurements allowed to determine an average of 217±32 molecules of **LD-LA** for each nanoparticle, in perfect agreement with previously published data on analogous lipoic acid derivatives [11]. The relatively high standard deviation

was essentially due to the small amount of sampled material and the presence of a low volatile solvent such as DMSO. The amount of adsorbed codrug obtained by TGA is five times higher than that obtained by HPLC-ESI-MS/MS technique. This difference could be imputed to the fact that some of the codrug molecules did not desorbe from the AuNPs during the chromatographic separation and therefore could not be detected by the ESI ionization mass spectrometry technique due to the high mass associated to each AuNP.

3.4. Stability of the gold nanoparticles

3.4.1. Stability in DMSO. The samples of gold nanoparticles obtained with various concentrations of the codrug were monitored for several months to assess their stability over the time. Table 4 reports the data of the samples obtained with **LD-DA** as the stabilizing agent. Data reported in Table 4 show that the obtained codrug-loaded nanoparticles were stable in DMSO. The best samples retained small sizes even after two months. In all the samples we noted a progressive absorbance decrease with time (see Supplementary data, Figure S10) as observed also in other similar studies [40]. Samples obtained with **DA-LA** were stable as well, although less stable than those obtained with **LD-LA** (See Supplementary data, Table S2).

Table 4. Stability over the time of the samples of gold nanoparticles obtained with **LD-LA** prepared at constant concentration of $HAuCl_4$ (1 mM) and $NaBH_4$ (1.5 mM) and increasing concentration of the codrug.

[**LD-LA**] (mM)		Size[a] (nm)					
Entry		0 d	7 d	21 d	49 d	77 d	100 d
1	0.10	5.9	5.3	58.1	59.9	69.3	Ppt.
2	0.25	5.8	6.2	17.7	63.8	77.8	81.6
3	0.50	6.7	6.3	6.3	5.9	23.3	64.6
4	0.75	4.2	5.5	31.9	131	Ppt.	Ppt.
5	1.00	4.2	5.8	4.6	24.0	19.2	53.4
6	1.50	7.0	5.6	3.4	76.7	93.4	78.9
7	2.00	5.3	7.9	6.1	46.9	48.6	50.7

8	3.00	5.2	5.4	10.3	41.6	73.9	Ppt.
9	5.00	5.4	10.1	15.9	20.1	196	Ppt.

[a] Determined by DLS.

3.4.2. Stability in phosphate buffer. The sample of **LD-LA**/AuNPs obtained with $HAuCl_4$ 1 mM, $NaBH_4$ 1.5 mM and **LD-LA** 1 mM was diluted 1:10 with phosphate buffer and its stability was monitored over the time using UV-vis spectrophotometric measurements (Figure S11 in the Supplementary data) and DLS (Table S3 in the Supplementary data). **LD-LA**/AuNPs were relatively poorly stable in PBS and a precipitate could be easily visualized after 30 minutes in the cuvette. This datum is in perfect agreement with the release profile of **LD-LA**/AuNPs after incubation in the PBS at pH 7.4 (see Figure 6 below). As a matter of fact the release of the stabilizing agent **LD-LA** caused the destabilization of AuNPs and favoured their precipitation. It is important to highlight that, due to the aggregation of AuNPs consequent to the release of the stabilizing agent, different populations of aggregates were monitored. In order to follow the low scattering of small AuNPs compared to bigger aggregated ones, Table S3 in the Supplementary data reports DLS distributions based on both intensity and number.

3.4.3. Stability in fetal bovine serum. The sample of **LD-LA**/AuNPs obtained with $HAuCl_4$ 1 mM, $NaBH_4$ 1.5 mM and **LD-LA** 1 mM was diluted 1:10 with BFS and its stability was monitored over the time by using DLS. As a matter of fact the presence of proteins in the serum did not allow to investigate this sample by using UV-vis spectrophotometry. In the presence of serum the nanoparticles demonstrated to be stable for days and no precipitate was evidenced (Figure 5). In this case serum proteins took the place of the released **LD-LA**, thus favouring the dispersion of AuNPs and avoiding their precipitation, although an increase of their dimension was observed on proteins/**LD-LA** substitution. It is important to highlight that due to the presence of proteins DLS analysis monitored different particulate populations also in the blank sample. In order to monitor the smallest objects, i.e. AuNPs, Table S4 in the Supplementary data reports DLS distributions based on both monomodal and multimodal size distribution.

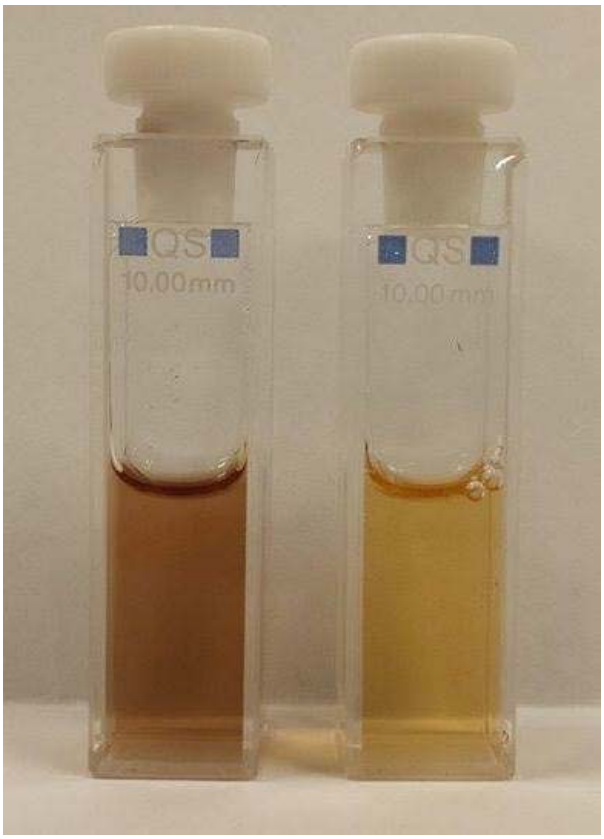

Figure 5. Samples of gold nanoparticles obtained from $HAuCl_4$ 1 mM, $NaBH_4$ 1.5 mM and 1 mM **LD-LA** by diluting the sample 1:10 (left sample) and 1:100 (right sample) with fetal bovine serum, 24 h after the dilution.

3.5. LD-LA release profile in phosphate buffer

Figure 6 shows the release profile of **LD-LA**/AuNPs after incubation in the phosphate buffer at pH 7.4. In particular, after 10 min and 1 h of incubation the percentage of released codrug was about 60% and 100%, respectively, suggesting that **LD-LA** molecules interact weakly with the surface of the gold nanoparticles, as previously evidenced [30,31].

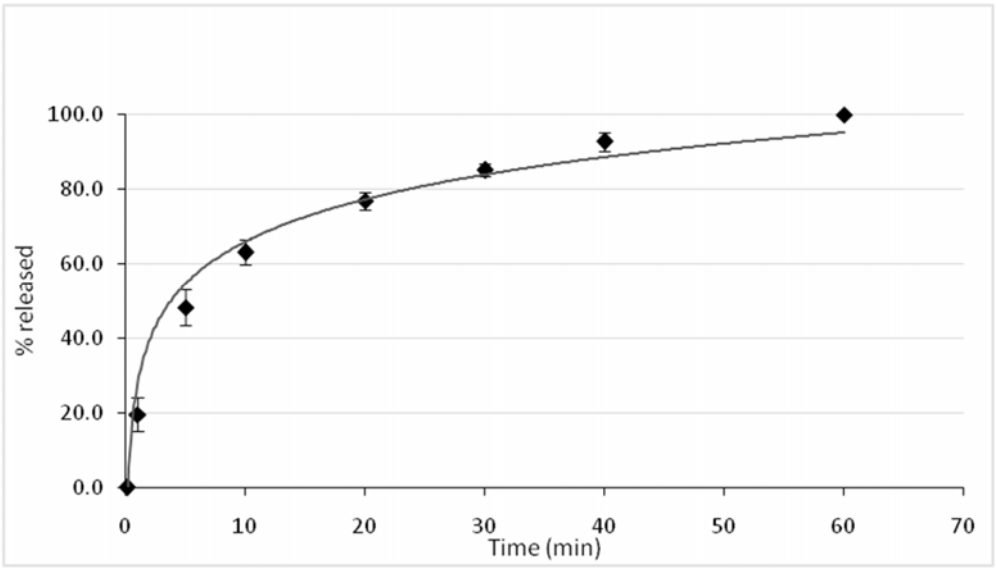

Figure 6. Release profile of **LD-LA**/AuNPs in PBS pH 7.4. Each values is the mean ± SD of three measurements.

3.6. Biocompatibility and biosafety of gold nanoparticles

At present, almost no standard biocompatibility evaluation criteria have been established for codrugs hybridized with nanoparticles. Hence, in this study, the cytotoxicity of the codrugs and of the codrugs hybridized with AuNPs was examined in human neuroblastoma cell line SH-SY5Y reported to be a valuable cellular model for studying neurotoxicity [41,42] and in peripheral cells, namely human primary whole-blood and isolated lymphocyte cultures. The effect of increasing concentrations of **LD-LA** and **DA-LA** on SH-SY5Y cell culture viability is shown in Figure 7. Following a 24 h drug exposure the release of the cytosolic enzyme LDH in the medium, reflecting cell death, resulted to be significant beginning from 100 μM with a calculated IC_{50} = 87 μM and 96 μM for **LD-LA** and **DA-LA,** respectively.

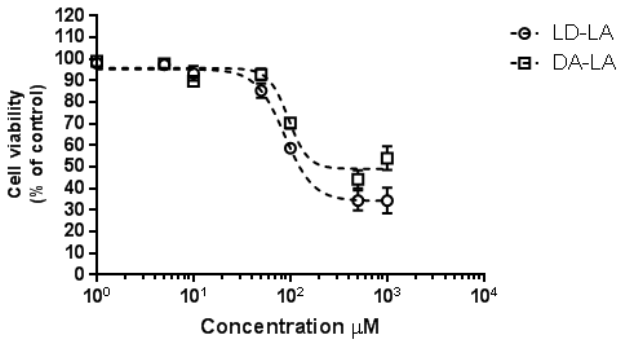

Figure 7. Cytotoxic effect of **LD-LA** and **DA-LA** (1-1000 μM) in neuroblastoma SH-SY5Y cells. LDH activity in the medium was detected after 24h treatment. The values are reported as percentage of the control (100% vitality). Each value is the mean ± SEM of at least three different set of experiments performed in duplicate.

Given the results on hydrolysis of the codrug, it was then chosen to perform further experiment by using **LD-LA, LD-LA**/AuNPs and **LD** (this latter as reference compound). The treatments were added to the cell medium for 24 and 48 h at different concentrations (1-1000 μM) and the cytotoxicity was measured by the classical LDH and MTT assays.

As reported in Figures 8a and 8b, no significant increase in LDH release was reported when SH-SY5Y cells were treated with all the compounds tested up to 50 μM. When higher concentrations were used (100 μM) **LD-LA** and **LD** caused an increase in LDH release whereas **LD-LA**/AuNPs resulted to be not cytotoxic. The hybrid codrug was toxic when added to the culture medium at higher concentration. Similar results were obtained by using MTT assay at 24 h as shown in Figure S12a. in the Supplementary data. When MTT assay was performed following a 48 h treatment also 100 μM **LD-LA**/AuNPs resulted to reduce cell viability by approximately 30% (see Figure S12b).

These results were consistent with those observed by brightfield images of the cells treated with **LD-LA**/AuNPs (1-1000 μM) for 24 and 48 h (see Figures S13 and S14 in the Supplementary data).

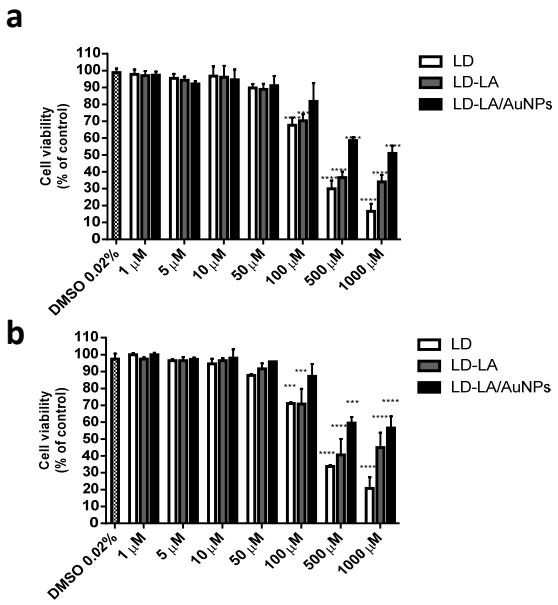

Figure 8. Cytotoxicity evaluation of **LD**, **LD-LA**, **LD-LA**/AuNPs (1-1000 μM) on neuroblastoma SH-SY5Y cells. f LDH activity in the medium was detected after 24 (a) and 48 h. (b) treatment. The values are reported as percentage of the control (100% vitality) according to the manufacturer's instructions. Each value is the mean ± SEM of at least three different set of experiments performed in duplicate. LDH release after treatments with vehicle (DMSO 0.02%) for 24 - 48h was 98.80% ± 2.36% and 97.36% ± 3.25% respectively . *P < 0.05, **P< 0.05, ***P< 0.001, ****P< 0.0001 compared to DMSO (0,02%) treated cells.

It is known that **LD** can induce the production of several cytotoxic oxygen radical species including semiquinones, quinones and hydrogen peroxide [43,44]. To investigate the effect of **LD, LD-LA** and **LD-LA**/AuNPs on the production of cytotoxic oxygen radical species, the accumulation of ROS in SH-SY5Y cells was measured utilizing the conversion of DCF-DA to DCF.

LD-LA and **LD** induced a significant increase in ROS levels compared to the untreated cells only starting from the concentration of 100 μM, whereas **LD-LA**/AuNPs caused a rise in ROS production only at higher concentration (500 μM). Interestingly, as shown in Figure 9 the conjugation of **LD** with **LA** resulted in a lower ROS production when compared to **LD**. The effect was even greater when the codrug was hybridized with AuNPs, indicating that **LA** keep its antioxidant activity even when bound to AuNPs.

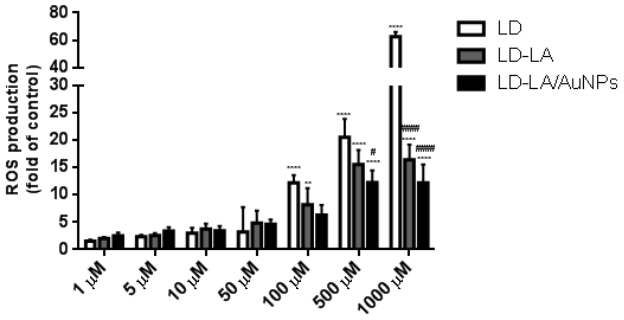

Figure 9. Effect of **LD**, **LD-LA**, **LD-LA**/AuNPs (1-1000 μM) on ROS production in neuroblastoma SH-SY5Y cell. The cells were stained with DCFDA and the treatments were carried out for 24 h. The values are reported as fold of the control according to the manufacturer's instructions. Each value is the mean ± SEM of at least three different set of experiments performed in duplicate. LDH release after treatments with vehicle (DMSO 0.02%) was 96.31% ± 1.26%. #P < 0.05, ##P< 0.0, ###P< 0.001, ####P< 0.0001 for **LD-LA** or **LD-LA**/AuNPs compared to LD at the same concentration *P < 0.05, **P< 0.05, ***P< 0.001, ****P< 0.0001 compared to control.

Besides its role within the brain, the dopaminergic system has been recently identified in other tissues and cell types including peripheral blood lymphocytes which represents a cellular model where: i) to test novel pharmacological approach to PD and other neurodegenerative and/or neuropsychiatric disorders; ii) to evaluate the systemic oxidative stress related to CNS treatment and diseases [45,46]. Thus, the cultures of human blood cells were exposed to different concentrations of **LD-LA**/AuNPs and **LD-LA** for 24 h and 48 h and cytotoxicity was measured by MTT and LDH assays. As shown in Figure 10, no obvious cytotoxicity against human blood cells was found for the **LD-LA**/AuNPs and **LD-LA** even at the high concentration of 100 μg/mL.

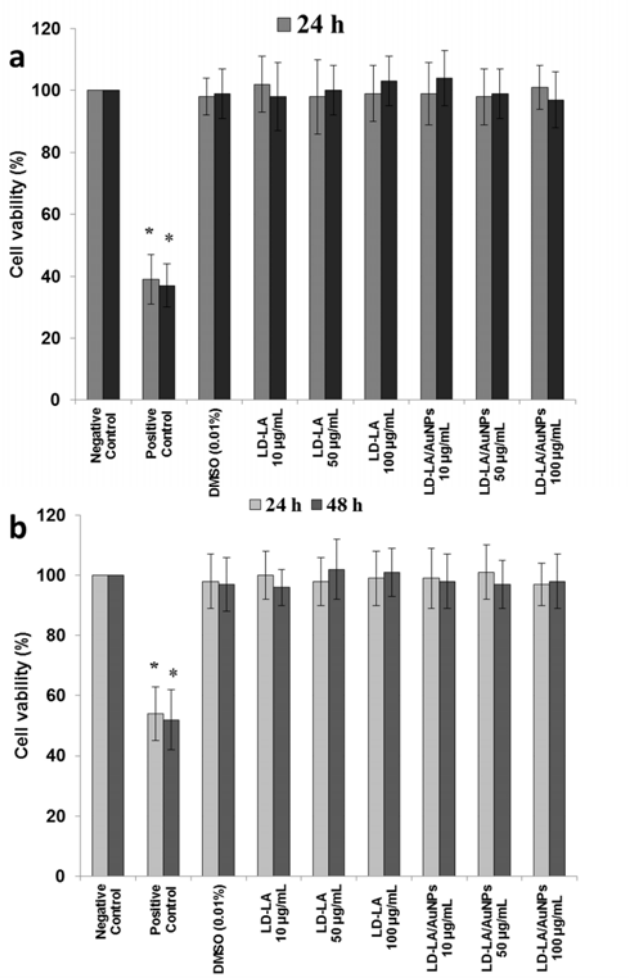

Figure 10. Results of the MTT assay of mitochondrial activity (a) and lactate dehydrogenase (LDH) release (b) in dividing human blood cells exposed to **LD-LA** and **LD-LA**/Au-NPs as a function of concentration and incubation time. * symbol presents the statistical difference from the negative control at the level of $p<0.05$.

We also focused on the oxidative effect induced by **LD-LA**/AuNPs by determining TAC and TOS levels commonly used to evaluate the systemic oxidative status [47]. Likewise, as reported in Table 5, **LD-LA**/AuNPs and **LD-LA** exposure did not change TOS levels in cultured human blood cells at all the investigated concentrations.

Table 5. TAC and TOS levels in cultured human blood cells maintained 24 and 48 h in the presence of **LD-LA**/AuNPs and **LD-LA**.[a]

Treatment	TAC as Trolox Equiv. (μmol L^{-1})		TOS as H_2O_2 Equiv. (μmol L^{-1})	
	24 h	48 h	24 h	48 h
Negative control	0.9±0.2^{a}	0.8±0.1^{a}	3.8±0.4^{a}	3.8±0.4^{a}
Positive control	2.0±0.4^{c}	2.2±0.3^{c}	9.2±0.7^{b}	9.4±0.5^{b}
LD-LA 10 μg/mL	1.2±0.1^{b}	1.2±0.2^{b}	3.4±0.5^{a}	3.8±0.4^{a}
LD-LA 50 μg/mL	1.3±0.3^{b}	1.4±0.2^{b}	3.7±0.3^{a}	3.8±0.6^{a}
LD-LA 100 μg/mL	1.6±0.3^{bc}	1.5±0.4^{b}	3.7±0.5^{a}	4.0±0.2^{a}
LD-LA/AuNPs 10 μg/mL	1.3±0.2^{b}	1.2±0.3^{b}	3.6±0.4^{a}	3.9±0.5^{a}
LD-LA/AuNPs 50 μg/mL	1.1±0.2^{b}	1.2±0.1^{b}	3.5±0.5^{a}	3.9±0.4^{a}
LD-LA/AuNPs 100 μg/mL	1.3±0.2^{b}	1.2±0.2^{b}	3.8±0.6^{a}	4.1±0.4^{a}

[a]Different superscripts, i.e. *a*,*b* and *c*, denote significant differences within each table column at the $p<0.05$ level. Values are expressed as means ± standard deviations of four experiments.

The lack of any noticeable toxicity of **LD-LA**/AuNPs at concentrations comparable or even higher to those reported to be reached in the plasma of patients treated with **LD** alone or in combination with catechol-O-methyltransferase (COMT) inhibitors [48,49] provides new opportunities for the safe application of these gold nanoparticles in drug delivery.

4. Conclusions

Gold nanoparticles can be used as carriers for **LD-LA** codrug because this molecule has proven to be an excellent stabilizing agent in the synthesis of such nanosystems and to be completely released from the NPs after 1 h. From UV-vis spectroscopy **DA-LA** appeared to be more easily hydrolyzed with respect to **LD-LA** and thus it was not investigated further as drug delivery vehicle.

The synthetic protocol developed is simple, versatile, gives good yields and is able to provide solutions of really small nanoparticles, quite stable over time in both DMSO and serum.

The present strategy definitely paves the way for the preparation of **LD-LA**/AuNPs with good biocompatibility towards both SH-SY5Y cells and cultured lymphocytes thus providing a novel and promising platform for the study of the biological applications of gold nanoparticles. Very interestingly, the **LD-LA**/AuNPs demonstrated to decrease ROS production of SH-SY5Y cells when compared to both **LD** and **LD-LA** and to not change TOS levels in cultured lymphocytes. The investigation of these nanosystems as alternative transporters of **LD-LA** in the treatment of diseases such as Alzheimer's and Parkinson's is therefore worth continuing overall considering the possibility to exploit the capacity of **LD** to activate specific transporters of the neuronal cells and thus favour BBB crossing.

Acknowledgements

We thank Dr. Erika Maria Di Meo and Dr. Piera Sozio for preliminary measurements regarding the optimization of the preparation protocol and the quantification of the drug as well as the synthesis of the codrug, respectively. This work was carried out with support from the Universities 'G. d'Annunzio' of Chieti-Pescara and MIUR (PRIN 2010-11, prot. 2010N3T9M4). A.D.C. thanks MIUR (PRIN 2010-11, prot. 2010N3T9M4) that funded his biennial postdoctoral fellowships.

Supplementary data: UV-vis spectra of codrugs in the absence and in the presence of $NaBH_4$; spectra of **LD** and **DA**; UV-vis spectra of AuNP stabilized by **DA-LA**; LC-MS analysis; TGA assays, stability measurements of **DA-LA**/AuNP in DMSO and of **LD-LA**/AuNPs in PBS and serum, citotoxicity (MTT test) on SH-SY5Y cells, Hematoxylin/Eosin SH-SY5Y cell staining.

References

[1] Sozio P, Iannitelli A, Cerasa L C, Cacciatore I, Cornacchia C, Giorgioni G, Ricciutelli M, Nasuti C, Cantalamessa F and Di Stefano A 2008 New L-dopa Codrugs as Potential Antiparkinson Agents *Arch. Pharm.* **341** 412-417.

[2] Di Stefano A, Sozio P, Cocco A, Iannitelli A, Santucci E, Costa M, Pecci L, Nasuti C, Cantalamessa F and Pinnen F 2006 L-Dopa- and Dopamine-(R)-α-Lipoic Acid Conjugates as Multifunctional Codrugs with Antioxidant Properties *J. Med. Chem.* **49** 1486-1493.

[3] Smith A R, Shenvi S V, Widlansky M, Suh J H and Hagen T M 2004 Lipoic Acid as a Potential Therapy for Chronic Diseases Associated with Oxidative Stress. *Curr. Med. Chem.* **11** 1135-1146.

[4] Zhang H, Jia H, Liu J, Ao N, Yan B, Shen W, Wang X, Li X, Luo C and Liu J 2010 Combined R-α-lipoic Acid and Acetyl-L-carnitine Exerts Efficient Preventative Effects in a Cellular Model of Parkinson's Disease *J. Cell. Mol. Med.* **14** 215-225.

[5] Sau S, Agarwalla P, Mukherjee S, Bag I, Sreedhar B, Pal-Bhadra M, Patra CR, Banerjee R 2014 Cancer cell-selective promoter recognition accompanies antitumor effect by glucocorticoid receptor-targeted gold nanoparticle *Nanoscale* **6** 6745-6754.

[6] Mukherjee S, Sau S, Madhuri D, Bollu VS, Madhusudana K, Sreedhar B, Banerjee R, Patra CR Green Synthesis and Characterization of Monodispersed Gold Nanoparticles: Toxicity Study, Delivery of Doxorubicin and Its Bio-Distribution in Mouse Model *J. Biomed. Nanotechnol.* **12** 165-181.

[7] Boisselier E and Astruc D 2009 Gold Nanoparticles in Nanomedicine: Preparations, Imaging, Diagnostics, Therapies and Toxicity *Chem. Soc. Rev.* **38** 1759-1782.

[8] Murphy C J, Gole A M, Stone J W, Sisco P N, Alkilany A M, Goldsmith E C and Baxter S 2008 Gold Nanoparticles in Biology: Beyond Toxicity to Cellular Imaging *Acc. Chem. Res.* **41** 1721-1730.

[9] Giersig M and Mulvaney P 1993 Preparation of Ordered Colloid Monolayers by Electrophoretic Deposition *Langmuir* **9** 3408-3413.

[10] Abad J M, Mertens S F L, Pita M, Fernández V M and Schiffrin D J 2005 Functionalization of Thioctic Acid-Capped Gold Nanoparticles for Specific Immobilization of Histidine-Tagged Proteins *J. Am. Chem. Soc.* **127** 5689-5694.

[11] Saada M-C, Montero J-L, Vullo D, Scozzafava A, Winum J-Y and Supuran C T 2011 Carbonic Anhydrase Activators: Gold Nanoparticles Coated with Derivatized Histamine, Histidine, and Carnosine Show Enhanced Activatory Effects on Several Mammalian Isoforms *J. Med. Chem.* **54** 1170-1177.

[12] Oh E, Susumu K, Goswami R and Mattoussi H 2010 One-Phase Synthesis of Water-Soluble Gold Nanoparticles with Control over Size and Surface Functionalities *Langmuir* **26** 7604-7613.

[13] Stewart M H, Susumu K, Mei B C, Medintz I L, Delehanty J B, Blanco-Canosa J B, Dawson P E and Mattoussi H 2010 Multidentate Poly(ethylene glycol) Ligands Provide Colloidal Stability to Semiconductor and Metallic Nanocrystals in Extreme Conditions *J. Am Chem. Soc*. **132** 9804-9813.

[14] Legname G A, Kroll S and Costa De Sousa M F 2010 Gold Nanoparticles Coated with Polyelectrolytes and Use Thereof as Medicament for the Treatment of Neurodegenerative Diseases Caused by Protein Aggregates Int. Pat. Appl. 2010052665 A2 May 14.

[15] D'Aurizio E, van Nostrum C F, van Steenbergen M J, Sozio P, Siepmann F, Siepmann J, Hennink W E and Di Stefano A 2011 Preparation and characterization of poly(lactic-co-glycolic acid) microspheres loaded with a labile antiparkinson prodrug *Int. J. Pharm*. **409** 289-296.

[16] Li S, Hou D, Sun M, Ping Q, Xu Y 2009 Preparation of freeze-dried chitosan-liposome containing L-dopa and pharmacokinetics in rats after oral administration *J. Pharm. China Univ.* **40** 406-411.

[17] Fontana A, Viale M, Guernelli S, Gasbarri C, Rizzato E, Maccagno M, Petrillo G, Aiello C, Ferrini S, Spinelli D 2010 Strategies for improving the water solubility of new antitumour nitronaphthylbutadiene derivatives *Org. Biomol. Chem*. **8** 5674–5681.

[18] Kageyama T, Nakamura M, Matsuo A, Yamasaki Y,Takakura Y, Hashida M, Kanai Y, Naito M, Tsuruo T, Minato N and Shimohama S 2000 The 4F2hc/LAT1 complex transports L-DOPA across the blood-brain barrier. *Brain Res.* **879** 115-121.

[19] Ravani L, Sarpietro M G, Esposito E, Di Stefano A, Sozio P, Calcagno M, Drechsler M, Contado C, Longo F, Giuffrida M C, Castelli F, Morari M and Cortesi R 2014 Lipid nanocarriers containing a Levodopa prodrug with potential antiparkinsonian activity *Mat. Sci. Eng. C-Mat.* **48** 294-300.

[20] Verger ML-L, Fluckiger L, Kim Y-I, Hoffman M, Maincent P 1998 Preparation and characterization of nanoparticles containing an antihypertensive agent *Eur. J Pharm. Biopharm*. **46** 137-143.

[21] Laserra S, Basit A, Sozio P, Marinelli L, Fornasari E, Cacciatore I, Ciulla M, Türkez H, Geyikoglu F, Di Stefano A 2015 Solid lipid nanoparticles loaded with lipoyl-memantine codrug: Preparation and characterization *Int. J. Pharm*. **485** 183-191.

[22] Evans H J and O'Riordan M L 1975 Human Peripheral Blood Lymphocytes for the Analysis of Chromosome Aberrations in Mutagen Tests *Mutat Res.* **31** 135-148.

[23] World Medical Assembly, Medical Ethics Committee 1999 Updating the WMA Declaration of Helsinki. *World Med. J.* **45** 11-13.

[24] Giuliani P, Romano S, Ballerini P, Ciccarelli R, Petragnani N, Cicchitti S, Zuccarini M, Jiang S, Rathbone M P, Caciagli F and Di Iorio P 2012 Protective activity of guanosine in an in vitro model of Parkinson's disease *Panminerva Med.* **54** 43-51.

[25] Porter L A, Ji D, Westcott S L, Graupe M, Czernuszewicz R S, Halas N J and Lee T R 1998 Gold and Silver Nanoparticles Functionalized by the Adsorption of Dialkyl Disulfides *Langmuir* **14** 7378-7386.

[26] Brust M, Walker M, Bethell D, Schiffrin D J and Whyman R J 1994 Synthesis of Thiol-derivatized Gold Nanoparticles in a Two-phase Liquid-liquid System *J. Chem. Soc., Chem. Commun.* 801-802.

[27] Brust M, Fink J, Bethell D, Schiffrin D J and Kiely C J 1995 Synthesis and Reactions of Functionalized Gold Nanoparticles *J. Chem. Soc., Chem. Commun.* 1655-1656.

[28] Brown W D 1960 Reduction of protein disulfide bonds by sodium borohydride *Biochim. Biophys. Acta*, **44** 365-367.

[29] Ookawa A, Yokoyama S and Soai K 1986 Chemoselective Reduction of Diaryl Bisulfides to Thiols with Sodium Borohydride in Mixed Solvent Containing Methaxol *Synthetic Commun*. **16**, 819-825.

[30] Grölnbeck H, Curioni A and Andreoni W 2000 Thiols and Disulfides on the Au(111) Surface: The Headgroup-Gold Interaction *J. Am. Chem. Soc*. **122** 3839-3842.

[31] Nuzzo R G, Zegarski B R and Dubois L H 1987 Fundamental Studies of the Chemisorption of Organosulfur Compounds on Gold(111). Implications for Molecular Self-assembly on Gold Surfaces *J. Am. Chem. Soc.* **109** 733-740.

[32] Cingolani G M, Di Stefano A, Mosciatti B, Napolitani F, Giorgioni G, Ricciutelli M and Claudi F. 2000 Synthesis of L-(+)-3-(3-Hydroxy-4-pivaloyloxybenzyl)-2,5-diketomorpholine as Potential Prodrug of L-Dopa *Bioorg. Med. Chem. Lett.* **10** 1385-1388.

[33] Strickley R G 2004 Solubilizing Excipients in Oral and Injectable Formulations *Pharm. Res.* **21** 201-230.

[34] Ansar S M, Ameer F S, Hu W, Zou S, Pittman C U and Zhang D 2013 Removal of Molecular Adsorbates on Gold Nanoparticles Using Sodium Borohydride in Water *Nano Lett.* **13** 1226-1229.

[35] Zhong Z, Patskovskyy S, Bouvrette P, Luong J H T and Gedanken A 2004 The Surface Chemistry of Au Colloids and Their Interactions with Functional Amino Acids *J. Phys. Chem. B* **108** 4046-4052.

[36] Okamoto T, Yamaguchi I, Kobayashi T 2000 Local plasmon sensor with gold colloid monolayers deposited upon glass substrates *Opt. Lett.* 25, 372-374.

[37] Haiss W, Thanh N, Aveyard J and Fernig D 2007 Determination of Size and Concentration of Gold Nanoparticles from UV-Vis Spectra *Anal. Chem.* ***79*** 4215-4221.

[38] Ríos-Corripio M A, García-Pérez B E, Jaramillo-Flores M E, Gayou V L and Rojas-López M 2013 UV-Visible intensity ratio (aggregates/single particles) as a measure to obtain stability of gold nanoparticles conjugated with protein A *J. Nanopart. Res.* **15** 1624/1-1624/7.

[39] Schlenoff J B, Li M and Ly H 1995 Stability and Self-Exchange in Alkanethiol Monolayers *J. Am. Chem. Soc.* **117**, 12528-12536.

[40] Mohd Sultan N and Johan M 2014 Synthesis and Ultraviolet Visible Spectroscopy Studies of Chitosan Capped Gold Nanoparticles and Their Reactions with Analytes *Sci. World J.* **2014**, 184604/1-184604/7.

[41] Cheung Y T, Lau W K, Yu M S, Lai C S, Yeung S C, So K F and Chang R C 2009 Effects of all-trans-retinoic acid on human SH-SY5Y neuroblastoma as in vitro model in neurotoxicity research *Neurotoxicology* **30** 127-135.

[42] Schule B, Pera R A and Langston J W 2009 Can cellular models revolutionize drug discovery in Parkinson's disease? *Biochim. Biophys. Acta-Mol. Basis Dis.* **1792**, 1043-1051.

[43] Lee J J, Kim Y M, Yin S Y, Park H D, Kang M H, Hong J T and Lee M K 2003 Aggravation of L-DOPA-induced neurotoxicity by tetrahydropapaveroline in PC12 cells *Biochem. Pharmacol*. **66** 1787-1795.

[44] Pedrosa R and Soares-da-Silva P 2002 Oxidative and non-oxidative mechanisms of neuronal cell death and apoptosis by L-3,4-dihydroxyphenylalanine (L-DOPA) and dopamine *Br. J. Pharmacol*. **137** 1305-1313.

[45] Buttarelli F R, Fanciulli A, Pellicano C and Pontieri F E 2011 The dopaminergic system in peripheral blood lymphocytes: from physiology to pharmacology and potential applications to neuropsychiatric disorders *Curr. Neuropharmacol*. **9** 278-288.

[46] Kokkinou I, Nikolouzou E, Hatzimanolis A, Fragoulis E G and Vassilacopoulou D 2009 Expression of enzymatically active L-DOPA decarboxylase in human peripheral leukocytes *Blood Cells Mol. Dis*. **42** 92-98.

[47] Aldemir M, Karaguzel E, Okulu E, Gudeloglu A, Ener K, Ozayar A and Erel O 2015 Evaluation of oxidative stress status and antioxidant capacity in patients with renal cell carcinoma *Cent. Eur. J. Urol*. **68**, 415-420.

[48] Dutton J, Copeland L G, Playfer J R and Roberts N B 1993 Measuring L-dopa in plasma and urine to monitor therapy of eldery patients with Parkinson disease treated with L-dopa and a dopa decarboxylase inhibitor *Clin. Chem*. **39**, 629-634.

[49] Blandini F, Nappi G, Fancellu R, Mangiagalli A, Samuele A, Riboldazzi G, Calandrella D, Pacchetti C, Bono G and Martignoni E 2003 Modifications of plasma and platelet levels of L-DOPA and its direct metabolites during treatment with tolcapone or entacapone in patients with Parkinson's disease *J. Neural. Transm*. **110**, 911-922.